

# Studying thermal transport in NSTX L and H-mode Plasmas with Global Gyrokinetic Simulation

EX-C

Y. Ren<sup>1</sup>, W. Wang<sup>1</sup>, W. Guttenfelder<sup>1</sup>, S.M. Kaye<sup>1</sup>, S. Ethier<sup>1</sup>, R.E. Bell<sup>1</sup>, B.P. LeBlanc<sup>1</sup>, E. Mazzucato<sup>1</sup>, D.R. Smith<sup>2</sup>, C.W. Domier<sup>3</sup>, H. Yuh<sup>4</sup> and the NSTX-U Team

<sup>1</sup>Princeton Plasma Physics Laboratory, Princeton University, Princeton, NJ 08543

<sup>2</sup>University of Wisconsin-Madison, Madison, WI, 53706

<sup>3</sup>University of California at Davis, Davis, CA 95616

<sup>4</sup>Nova Photonics, Inc., Princeton, NJ 08540

First-principle gyrokinetic simulations play an important role in studying the relation between plasma turbulence and anomalous thermal transport. In order to predict the confinement performance of future devices, it is crucial to validate gyrokinetic codes against experiments. Nonlinear local gyrokinetic simulations have been used to assess turbulence-driven transport in NSTX L and H-mode plasmas [1,2], and agreement in thermal transport with experiments has only been observed in limited cases. Due to the larger  $\rho^*$  of NSTX ( $\rho^* \sim 0.01$ ) compared to conventional tokamaks, global effects may be important in determining thermal transport [3]. Here we report studies of thermal transport in NSTX L and H-mode plasmas using the global particle-in-cell Gyrokinetic Tokamak Simulation (GTS) code [4].

Fast response of electron-scale turbulence to auxiliary heating cessation was observed in a set of RF-heated L-mode plasmas [5,6], where electron thermal transport is found to reduce by about a factor of 2 after the cessation of RF heating. Ion-scale global nonlinear gyrokinetic simulations are carried out with GTS code for  $t=465$  ms (with 1 MW injected

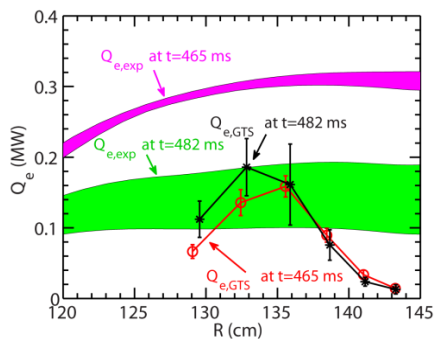


**Figure 1** Red circles: electron energy flux,  $Q_{e,GTS}$ , at  $t=465$  ms (before the RF cessation) as a function of major radius from nonlinear GTS simulation; black asterisks:  $Q_{e,GTS}$  at  $t=482$  ms (after the RF cessation) from nonlinear GTS simulation; magenta band: radial profile of experimental electron heat flux,  $Q_{e,exp}$ , at  $t=465$  ms from power balance analysis; green band: radial profile of  $Q_{e,exp}$  at  $t=482$  ms. Note that the vertical widths of the magenta and green bands denote the experimental uncertainties.  $Q_{e,GTS}$  is averaged over a quasi-steady saturation period, and the errorbars of  $Q_{e,GTS}$  are the standard deviation of  $Q_{e,GTS}$  in the averaging time period.

RF power) and for  $t=482$  (after the RF heating cessation) with experimental equilibrium profiles to assess global effects on electron thermal transport. These global simulations cover a radial domain from  $\Psi_N=0.25$  to  $0.8$  ( $R \sim 120$  cm to  $147$  cm), where  $\Psi_N$  is the square root of the normalized toroidal flux. The size of grids on poloidal planes is about local  $\rho_i$ , and 80 particles per cell-species are used. The experimental equilibrium  $E \times B$  shear is turned on from the beginning of the simulations. Figure 1 compares electron energy flux,  $Q_{e,GTS}$ , radial profiles at  $t=465$  and  $482$  ms from GTS simulations with the profiles of experimental electron heat flux,  $Q_{e,exp}$  at the same two time points. It can be clearly seen that while  $Q_{e,GTS}$  is essentially the same for both  $t=465$  ms (with RF heating) and for  $t=482$  ms (after the RF cessation) at  $R \gtrsim 136$  cm,  $Q_{e,GTS}$  at  $R \lesssim 134$  cm is larger at  $t=482$  ms than at  $t=465$  ms. The observed change in  $Q_{e,GTS}$  before and after the RF cessation is opposite to the change in experimental electron heat flux,  $Q_{e,exp}$ , from power balance analysis, i.e.  $Q_{e,exp}$  at  $t=465$  ms is about a factor of 2 higher than  $Q_{e,exp}$

$t=482$  ms. The GTS simulation result is consistent with our linear and nonlinear local simulations (not shown) that the observed equilibrium profile changes cannot explain the reduction in electron thermal transport. Thus we conclude that global effects from profile variation, e.g. turbulence spreading, are not likely able to explain the observed reduction in electron thermal transport. It is interesting that  $Q_{e,GTS}$  at  $t=465$  and  $482$  ms are both in good agreement with  $Q_{e,exp}$  at  $t=482$  ms (after the RF cessation) but not with  $Q_{e,exp}$  at  $t=482$  ms (with RF heating). These results imply that nonlocal flux-driven mechanism may be important for the observed electron thermal transport [7].

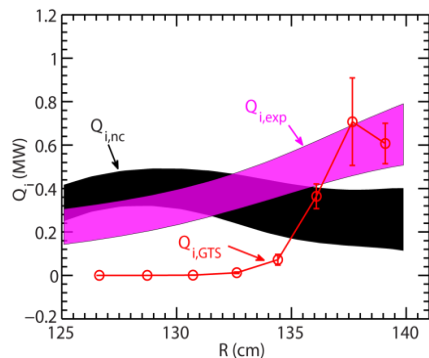


**Figure 2** Red circles: ion energy flux,  $Q_{i,GTS}$ , at  $t=332$  ms as a function of major radius from a nonlinear GTS simulation of an NSTX H-mode plasma, shot 141767; magenta band: radial profile of experimental ion heat flux,  $Q_{i,exp}$ , at  $t=332$  ms from power balance analysis; black band: radial profile of neoclassical ion heat flux,  $Q_{i,nc}$ . The same definition of uncertainties and errorbars applies as in Fig. 1.

GTS code has also been applied to NSTX H-mode plasmas. Here we present the results from an ion-scale GTS simulation of an NSTX H-mode plasma (shot 141767), where electron-scale turbulence is found to be reduced/stabilized by large electron density gradient [8]. Figure 2 compares ion energy flux,  $Q_{i,GTS}$ , radial profiles at  $t=332$  ms from the GTS simulation with experimental ion heat flux,  $Q_{i,exp}$ , radial profiles together with neoclassical ion heat flux,  $Q_{i,nc}$ , from NCLASS [9]. It can be seen that  $Q_{i,exp}$  is comparable to

$Q_{i,nc}$  at  $R \lesssim 132$  cm, which is consistent with the very small  $Q_{i,GTS}$ . At larger radius, i.e.  $R \gtrsim 136$  cm,  $Q_{i,GTS}$  is significantly larger than at smaller radius, consistent with  $Q_{i,exp}$  being significantly larger than  $Q_{i,nc}$ . In fact, considering the errorbars and uncertainties in  $Q_{i,GTS}$ ,  $Q_{i,exp}$  and  $Q_{i,nc}$ ,  $Q_{i,GTS} + Q_{i,nc}$  is approximately equal to  $Q_{i,exp}$ , showing that ion-scale turbulence is responsible for observed ion thermal transport. We note that  $Q_{e,GTS}$  is significantly smaller than  $Q_{e,exp}$  (not shown), which may be due to the possible contribution from ETG turbulence that is not captured by this ion-scale GTS simulation or electromagnetic effects which are not yet taken into account by GTS code.

In summary, we have applied global GTS simulations to NSTX L and H-mode plasmas. Agreement and disagreement in thermal transport between simulation and experiment have been observed. Further experimental and simulation explorations are needed to quantify the parametric regime where global effects are important. This work was supported by the U.S. Department of Energy under Contracts No. DE-AC02-76CH03073, No. DE-FG03-95ER54295, and No. DE-FG03-99ER54518. The computational resource is provided by NERSC.

- [1] Y. Ren et al., Phys. Plasmas 19, 056125 (2012)
- [2] Y. Ren et al., Nucl. Fusion 53, 083007 (2013)
- [3] W. X. Wang et al., Phys. Plasmas 17, 072511 (2010)
- [4] W. X. Wang et al., Phys. Plasmas 14, 072306 (2007)
- [5] Y. Ren et al., "Experimental Observation of Nonlocal Electron Thermal Transport in NSTX RF-heated L-mode plasmas", Proc. 25th Int'l. Atomic Energy Agency Fusion Energy Conference, EX/P6-43, St Petersburg, Russia Federation, October 13-18, 2014
- [6] Y. Ren et al., Phys. Plasmas 2, 110701 (2015)
- [7] S.-I. Itoh and K. Itoh, Sci. Rep. 2, 860 (2012)
- [8] J. Ruiz Ruiz et al., Phys. Plasmas 22, 122501 (2015)
- [9] W.A. Houlberg et al., Phys. Plasmas 4, 3230 (1997)